NWRI CONTRIBUTION #83-16

Tsang(47)

Pedrosa (2)

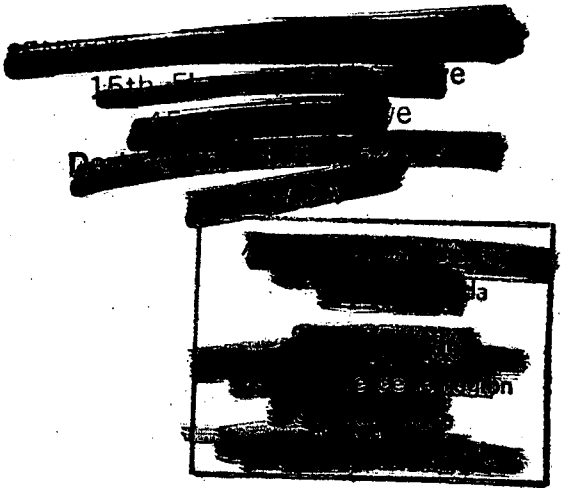

DEVELOPMENT AND CALIBRATION OF THE NWRI FRAZIL INSTRUMENT

By

Gee Tsang and Manuel Pedrosa

Environmental Hydraulics Section
Hydraulics Division
National Water Research Institute
Canada Centre for Inland Waters

October 1983

ABSTRACT

After 10 years of development, a frazil instrument capable of measuring the point concentration of frazil in flowing water has been produced and calibrated. The instrument is based on the theoretical principle that when ice is formed, impurities are rejected, frazil therefore may be considered as electrically non-conductive and its concentration in water can be measured by comparing the resistance of a sample of frazil-laden water with that of a sample of frazil-free water.

The instrument was calibrated in the laboratory. The calibration testing showed that the instrument performed satisfactorily. Because the frazil crystals are not isotropic, a calibration factor F greater than unity is involved. The division of the measured concentration by F gives the true concentration of frazil in water. F is a function of the flow velocity and turbulence and can be obtained through calibration.

RÉSUMÉ

Après 10 ans de perfectionnement, on a produit et calibré un frasimètre capable de mesurer la concentration de frasil en un point des eaux courantes. La conception de l'appareil repose sur le principe théorique voulant que lorsque de la glace se forme, les impuretés qu'elle contient sont rejetées, le frasil peut par conséquent être considéré comme électriquement non conducteur et sa concentration dans l'eau peut être mesurée en comparant la résistance d'un échantillon d'eau chargée de frasil avec celle d'un autre échantillon d'eau sans frasil.

L'appareil e été calibré en laboratoire. L'essai de calibration a démontré que le rendement de l'appareil était satisfaisant. Comme les cristaux de frasil ne sont pas isotropiques, un facteur de calibration F supérieur à l'unité a été employé. La division par F de la concentration mesurée donne la concentration réelle du frasil dans l'eau. F est une fonction de la vitesse du courant et de la turbulence, ce facteur peut donc être déterminé par calibration.

MANAGEMENT PERSPECTIVE

Frazil ice is produced by flowing water in the absence of an ice cover during the winter. This ice changes the available cross section availability for flow and may lead to flooding.

New winter navigation channels will create more frazil, changing the normal winter flow regions.

Up to now, the mass of ice produced was deduced by best budget assumption which were not verifiable. Moreover, the distribution and behaviour of the ice in the water channel is not known.

This new instrument opens up a way to understand the frazil ice in nature so that its effects and behaviour may be understood.

Results of studies will permit forecasts of the change in ice regime where developments are contemplated such as new power dams or winter navigation.

T. Milne Dick
Chief
Hydraulics Division

PERSPECTIVE DE GESTION

En hiver, le frasil est produit par l'eau courante lorsque celle-ci est dépourvue de couverture de glace. La glace modifie la coupe transversale disponible pour le courant et peut causer une inondation.

De nouveaux chenaux de navigation hivernale créeront davantage de frasil, ce qui modifiera les zones normales d'écoulement hivernal.

Jusqu'à ce jour, la masse de glace produite a été déterminée par déduction au moyen d'une "hypothèse de budget optimal" qui n'a pu cependant être vérifiée. En outre, on ne connaît toujours pas la répartition et le comportement de la glace dans la voie d'eau.

Ce nouvel appareil fournit un moyen de comprendre la nature du frasil afin de pouvoir expliquer ses effets et son comportement.

Le résultat des études permettra de faire des prévisions concernant les changements dans le régime des glaces où des progrès sont envisagés comme de nouveaux barrages hydroélectriques et la navigation hivernale.

Le chef de la Division de l'hydraulique
T. Milne Dick

TABLE OF CONTENTS

1.0 INTRODUCTION AND BACKGROUND

In turbulent water, whether in a flowing river or in an open lake, the ice formed is in the form of fine crystals suspended in the water and is known as frazil. Depending on the degree of super cooling and the salinity of the water, the crystallographic shape and evolution of the frazil vary. For fresh water under most natural conditions, however, the frazil is in the form of discoids that grow into dendritic crystals.

Frazil can greatly affect the flow properties of the flow. It can also adhere to underwater objects to form anchor ice. In both cases, the conveyancy capacity of a water course can be substantially reduced. When frazil adheres to submerged water intake structures, it often can completely block off the water intake and cause water supply or power production problems. In order to best utilize the water resources during winter months, one therefore should study the properties and effects of frazil on water flow.

The quantitative study of frazil in the past has been slow, due, to a large extent, to the lack of an instrument that can quantitatively measure the concentration of frazil in water. Before a major embarkment can be made in frazil research, the development of such an instrument is necessary.

Natural water is electrically conductive because of its mineral content. When water turns into ice, however, the impurities are rejected because the orderly arrangement of ice molecules does not permit impurity inclusion. For this reason ice crystals themselves are electrically non-conductive. Thus, by measuring the electrical resistance of a water-frazil mixture, the amount of frazil in the mixture can be evaluated. Kristinsson (1970) was the first person to construct an instrument using the above principle to measure frazil in a river. He wound two wires spirally on an insulator rod and immersed the rod in the river. By measuring the resistance between the two wires, the concentration of frazil over the depth of the rod was estimated. Also using the same principle but by measuring the increased

conductivity of the water because of salt rejection, Gilfillian et al (1972) were able to calculate the amount of ice formed in a river. Besides the electrical conductivity principle, frazil may also be measured with an instrument constructed based on the calorific principle as contemplated by Ford (1982) or the laser doppler principle as reported by Schmidt and Glover (1975) although a working instrument based on these two principles has yet to be developed.

To develop an instrument to measure the point concentration of frazil has long been identified as one of the priorities of frazil research by the Hydraulics Division, National Water Research Institute. The conceptual design of an instrument based on the conductivity principle for measuring point concentration of frazil as well as the velocities of the frazil packs and the flowing water was proposed by Tsang (1973) and the theoretical ground work guiding the design was given. An experimental instrument was later constructed and tested, which verified the soundness of the frazil-sensing physical principle. The work involved with the construction, testing and evaluation of the experimental instrument was known as Phase I of the frazil instrument development and was reported by Tsang (1977).

Encouraged by the Phase I work and following the "make or buy" policy, a contract was awarded to an external contractor to design and construct a manufacturable frazil instrument.The instrument subsequently produced turned out to be of a complex electronic design. It contained many components that were electronically interwoven and were controlled through the employment of a micro-processor. Although initial testing did indicate that the instrument appeared to be functioning, the accumulated handling and heating of the instrument because of ill ventilation soon led to short circuits and burning out of electronic components. Repairing and trouble-shooting were ineffectual because of the complex design and less than satisfactory construction and workmanship. Eventually it was decided that the instrument was no longer worth salvaging and a fresh start should be made to construct an instrument of rugged construction and practical design. The design and construction of the

instrument by the external contractor, its in-house testing, trouble-shooting, repairing and evaluation constituted Phase II of the instrument development and was reported by Tsang in detail (1982).

Three lessons were learned from the Phase II development of the instrument. The first was that the development of a finished instrument from proven physical principles alone in one step by an external contractor is unlikely to succeed because of the lack of interaction between the scientific authority, the designer and the manufacturer in view of the long feedback loop. The second lesson was that a good instrument should be simple in design and easy and cheap to trouble-shoot and repair. The third lesson was that the electrical heating of the instrument for deicing, although scientifically plausible, will likely cause trouble to the instrument in its actual use. The Phase II instrument was electrically heated by imbedded heating elements in the probes and in the supports. During the testing, the burnout of the heating elements was experienced both when the environment was warming up or cooling down. In the former case, such as the removal of the probe from the cold water, the heat generated by the heaters was not removed and started to build up around the heaters. Before the temperature build up was sensed by the temperature sensor some distance away and a signal was given to cut off the heater current, the heating elements had already been burned out. In the later case, such as the fast cooling of the water, because of the high heat flux lost to the environment, the heaters had to be at a high temperature to maintain the heat flow and this also resulted in burning out of the heaters. Because the temperature sensors and heaters were well imbedded in the probes and supports, their repair was difficult and expensive. As a rule, an expensive burned out probe would have to be written off completely. With the above experience, it was decided that for future instrument development, electrical heating for deicing should be avoided.

Following the unsuccessful attempt of the Phase II development, the physical working principle of the instrument was re-examined and reaffirmed. The temperature effect on the conductivity of water

was also studied. The work involved in this period is known as Phase III of the development and was reported by Ford et al (1981).

This report covers the last phase, or Phase IV of the development. As a result of this phase's work, a successful laboratory instrument was produced which could measure the point concentration of frazil in flowing water. Slight modification and adaptation of the instrument should make it suitable for field use. By measuring frazil concentration simultaneoulsy at two points one can study spatial correlation of frazil in the flow. Learning from the past, the Phase IV instrument was developed internally. A project team was assembled with clear functional role to each team members. Fast and frequent feedback was maintained throughout the project. The actual design, construction, testing, calibration and evaluation of the instrument and project write up were completed within two years.

Thus, after ten years, a working instrument was finally developed. This instrument will no doubt help to greatly increase human knowledge of frazil, especially after later improvement and refinement.

2.0 SCIENTIFIC PRINCIPLE OF FRAZIL SENSING

Because frazil is electrically non-conductive, its concentration in water can be measured by comparing the resistance of a sample of frazil-free water with that of frazil-laden water. This simple resistance or conductance comparison is the underlying scientific principle of the frazil instrument.

Let the water between a pair of insulated electrode plates be the water sample (see Fig. 1). The resistance between the electrodes is given by

$$R = \rho D/A \qquad (1)$$

where ρ is the resistivity of the water, D is the length of the electrical path and A is the area receiving the electrical lines. In case there are no frazil crystals nor other non-conductive particles in the water sample, D will be the distance between the two plates and A will be the area of one electrode plate.

The conductivity (or resistivity) of water is determined by the number of ions in it and the state of agitation of the ions. Because the former is determined by the salt content of the water and the latter is controlled by the temperature of the water, the resistivity of the water, therefore, should be a function of the following form:

$$\rho = f(S,T) \tag{2}$$

where S is the salt content and T is the temperature.

Salt content (not to be confused with salinity) is defined as the mass of salt per unit volume of solution. Because of the rejection of salt accompanying the formation of ice, the salt content of frazil-producing water should be continuously varying with time. If one denotes V_o as the total volume of the frazil/water mixture, V_f as the volume of the frazil and M_s as the mass of salts dissolved in the water part of the mixture, then the salt content of the water is given by

$$S = \frac{M_s}{V_o - V_f} \tag{3}$$

As the amount of frazil changes in the mixture, so will the salt content of the water.

The above equation can be rearranged to give

$$S = \frac{M_s/V_o}{1 - V_f/V_o} = \frac{S_i}{1 - \bar{c}_f} \tag{4}$$

or

$$\frac{S_i}{S} = 1 - \bar{c}_f \tag{5}$$

where $S_i = M_s/V_o$ is the initial salt content of the water before frazil is formed and $\bar{c}_f = V_f/V_o$ can be considered as the average volmetric concentration of frazil in the frazil/water mixture.

Because the conductivity of water is proportional to the number of ions in it or to the salt content of the water and resistivity is the reciprocal of conductivity, one therefore can write the following equations for the resistivity of the water:

$$\rho_{i(T)} = \text{Const.}/S_i \quad \text{and} \quad \rho_{(T)} = \text{Const.}/S \tag{6}$$

where T indicates the given temperature and subscript i indicates the initial condition before frazil is formed. From Eqs. 5 and 6, one obtains

$$\rho_{(T)} = (1 - \bar{c}_f)\ \rho_{i(T)} \tag{7}$$

The substitution of the above equation into Eq. 1 gives

$$R_{(T)} = (1 - \bar{c}_f)\ \rho_{i(T)} D/A \tag{8}$$

The above equation states that the resistance between the plates in Fig. 1 is affected by the temperature of the water and the average concentration of frazil in the water (even if frazil is excluded from the sample volume).

Although the electrode plates may be of any geometric shape, for easy comprehension and mathematical manipulation, they are assumed to be rectangular here with sides L_2 and L_3 and are L_1 apart. Call the probe for which the water sample is frazil-free the "reference probe", then for the reference probe the length of the electrical path will be L_1 and the electrical line receiving area will be L_2L_3. The resistance between the two electrode plates thus will be

$$R_{r(T)} = (1 - \bar{c}_f)\, \rho_{i(T)} L_1/(L_2L_3) \tag{9}$$

where the subscript r refers to the reference probe.

The probe for which frazil is present may be called the "sensor probe". For the sensor probe, the electrical path will be longer than L_1 because the electrical lines have to go around the frazil crystals on their way from one electrode to the other. If the sensed volume between the two electrodes is divided into many small tubes spanning from one electrode plate to the other with a cross-section area equal to the average size of the frazil crystals and the distribution of frazil crystals is assumed to be uniform, then for each tube there will be n crystrals for the electrical line to go around. Assuming that the frazil crystals are geometrically isotropic and the representative linear dimension of a frazil crystal is ℓ, then the length of the electrical path from one electrode plate to the other will be

$$D = L_1 + \Delta L_1 = L_1 + n\,(\xi\ell) = L_1(1 + n\,\xi\ell/L_1) \tag{10}$$

where ξ is the shape factor of the frazil crystals and $\Delta L_1 = n(\xi\ell)$

is the increase in electrical path length because of the presence of frazil crystals.

The presence of frazil crystals in the water also affects the electrical line receiving area of the electrodes. Fig. 2 shows an electrode plate covered with a layer of water of thickness ℓ. If this thin layer is divide into many vertical and horizontal tubes of width ℓ as shown in Fig. 2, then there will be m cyrstals per vertical tube and p crystals per horizontal tube and the receiving area of the electrode plate will be given by

$$A = (L_2 - m\xi\ell)(L_3 - p\xi\ell) = L_2L_3(1 - m\xi\ell/L_2)(1 - p\xi\ell/L_3) \quad (11)$$

Because of the uniform distribution assumption, one sees that

$$n/L_1 = m/L_2 = p/L_3 \quad (12)$$

or

$$\frac{n\xi\ell}{L_1} = \frac{m\xi\ell}{L_2} = \frac{p\xi\ell}{L_3} = \frac{\Delta L}{L} \quad (13)$$

The substitution of the above equation into Eqs. 10 and 11 gives

$$D = L_1\left(1 + \frac{\Delta L}{L}\right) \text{ and } A = L_2L_3\left(1 - \frac{\Delta L}{L}\right)^2 \quad (14)$$

and the substitution of the above equations into Eqs. 8 gives

$$R_{s(T)} = (1 - \bar{c}_f)\ \rho_{i(T)}\ \frac{L_1}{L_2\ L_3}\left[\frac{1 + \Delta\ L/L}{(1 - \Delta L/L)^2}\right] \quad (15)$$

where the subscript s indicates the sensor probe.

The quantity in the square bracket in the above equation can be related to the concentration of frazil in the probe. From

volumetric considerations one sees that the concentration of frazil in the probe can be calculated from

$$c_f = \frac{L_1 L_2 L_3 - (L_1 - n\xi\ell)\,(L_2 - m\xi\ell\,)(L_3 - p\xi\ell)}{L_1 L_2 L_3} \qquad (16)$$

where the first part of the numerator on the right hand side of the equation is the total sample volume and the second part is the volume of the water without the frazil. Because in most practically important cases, the concentration of frazil in water is small, seldom exceeding a few percent, $n\xi\ell$, $m\xi\ell$ and $p\xi\ell$ will be small compared with L_1 , L_2 and L_3 respectively. By expanding Eq. 16 and neglecting the higher order terms, one obtains

$$c_f = n\xi\ell/L_1 + m\,\xi\ell/L_2 + p\,\xi\ell\,/L_3 = 3\,\Delta L/L \qquad (17)$$

The substitution of the above equation in Eq. 15 leads to

$$R_{s(T)} = (1 - \bar{c}_f)\,\frac{(1 + c_f/3)}{(1 - c_f/3)^2}\,\frac{\rho_{i(T)} L_1}{L_2 L_3} \qquad (18)$$

$$R_{s(T)} = (1 - \bar{c}_f)\,\frac{(1 + c_f/3)}{(1 - c_f/3)^2}\,\frac{\rho_{i(T)} L_1}{L_2 L_3} \qquad (18)$$

It should be carefully noted that the above equation contains two frazil concentrations, $\bar{c}_f$ and c_f. While $\bar{c}_f$ is the average concentration of frazil of the frazil producing water, c_f is the concentration of frazil of the sampled volume in the sensor probe or the concentration of frazil at the measuring point. These two concentrations must not be confused.

It should be carefully noted that the above equation contains two frazil concentrations, $\bar{c}_f$ and c_f. While $\bar{c}_f$ is the average concentration of frazil of the frazil producing water, c_f is the concentration of frazil of the sampled volume in the sensor probe or the concentration of frazil at the measuring point. These two concentrations must not be confused.

$(1-c_f/3)^2$ in Eq. 18 may again be expanded and the higher order term of $c_f/3$ dropped because of its small magnitude. This will reduce Eq. 18 to

$(1-c_f/3)^2$ in Eq. 18 may again be expanded and the higher order term of $c_f/3$ dropped because of its small magnitude. This will reduce Eq. 18 to

$$R_{s(T)} = (1 - \bar{c}_f)\,\frac{(1 + c_f/3)}{(1 - 2c_f/3)}\,\frac{\rho_{i(T)} L1}{L_2 L_3} \qquad (19)$$

$$R_{s(T)} = (1 - \bar{c}_f)\,\frac{(1 + c_f/3)}{(1 - 2c_f/3)}\,\frac{\rho_{i(T)} L1}{L_2 L_3} \qquad (19)$$

The expression $1/(1 - 2c_f/3)$ may be expressed as a series of $2c_f/3$ and the higher order terms of $2c_f/3$ in this series may be once again ignored. Such an exercise will reduce the above equation to

$$R_{s(T)} = (1 - \bar{c}_f)(1 + c_f/3)(1 + 2c_f/3) \frac{\rho_{i(T)} L_1}{L_2 L_3} \qquad (20)$$

The above equation shows that the resistance of the sensor probe not only is affected by the concentration of frazil in the sensor probe, but also affected by the average concentration of frazil of the ambient water and the water temperature through its influence on $\rho_{i(T)}$. Because the temperature of the water may vary and the average concentration of frazil in the ambient water is also a function of the history of the water, to measure frazil concentration by measuring the resistance of the sensor probe alone, as was once contempleted by Ford et al (1981), should be difficult.

The above difficulty, however, can be eliminated easily if instead of measuring $R_{s(T)}$, one measures

$$\frac{R_{s(T)} - R_{r(T)}}{R_{r(T)}} \qquad (21)$$

The substitution of Eqs. 9 and 20 into the above expression, following the expansion of the multiplication factors and the dropping of the higher order c_f terms, immediately leads to

$$\frac{R_{s(T)} - R_{r(T)}}{R_{r(T)}} = c_f \qquad (22)$$

the concentration of frazil in the sensor probe.

From the above derivation, one sees that by measuring $(R_s - R_r)/R_r$, the concentration of frazil in water can be measured directly. Such a measurement is neither affected by the temperature of the water, nor by the amount of frazil that had formed in the ambient water. The employment of Eq. 22 for frazil sensing, however, requires that the water in the reference probe and in the sensing probe be of the same conductivity.

During the derivation of Eq. 22, the straying effect of the electrical lines in the probes has been ignored, the distribution of the frazil crystals has been assumed uniform and the geometric shapes of the frazil crystals have been assumed isotropic. The departure of the actual conditions from the above idealizations should affect the linearity of the relationship and require calibration. During the derivation, it was also assumed that the concentration of frazil is low. If this assumption is not observed, one should expect to see a non-linear relationship between $(R_s - R_r)/R_r$ and c_f. Nevertheless, a one to one relationship between $(R_s - R_r)/R_r$ and c_f should still exist. By calibration, one again should be able to measure the concentration of frazil under high frazil concentration conditions.

3.0 CONCEPTUAL DESIGN OF INSTRUMENT

Under the guidance of the theory shown in the last section and with the experience learned from previous phases of the instrument development, the conceptual design of the instrument as shown by Fig. 3 was conceived and adopted. It is seen from Fig. 3 that the conceptual design consists of two basic components; the component for frazil sensing, signal processing and signal display and the component for deicing. The frazil sensing and displaying component is shown by the upper part of the diagram. It is seen from this part of the diagram that the instrument has two probes; the sensor probe in which frazil is present and the reference probe in which frazil is

excluded. These two probes are identically constructed and in each probe, an identical A.C. current of constant strength flows between the electrode plates. These two constant A.C. currents are converted from two constant D.C. currents which are generated by two independent constant current sources, one for each probe. The reason to use A.C. current is to avoid polarization effects which otherwise will produce oxygen and hydrogen bubbles to block the electrode plates. To reduce the electro-chemical reactions, the frequency of the A.C. current is chosen to be high, but not high enough to cause excessive stress to the ions and to produce unwarranted capacitance leakeages. The strength of the current is also made small, but not too small as to hinder frazil sensing function of the instrument. The currents in the probes produce a voltage drop of $V_s = R_s I$ across the sensor probe and a voltage drop of $V_r = R_r I$ across the reference probe, I being the strength of the current. By feeding V_s and V_r to a voltage processor where the voltages are subtracted, divided and amplified, one obtains

$$G \frac{V_s - V_r}{V_r} = G \frac{R_s - R_r}{R_r} \tag{23}$$

where G is a dimensional gain factor. According to Eq. 22, one sees that the above signal is the concentration of frazil in the sensor probe multiplied by the dimensional gain factor G.

Three ways are provided to display or further processing the analog signal from the voltage processor. The first is to record the signal with an external tape recorder for later analysis. The second is to record the signal with a chart recorder that is built-in to the instrument and the third is to integrate the signal with an integrator. The reference voltage or the base voltage of the integrator can be changed by means of an external reference voltage source. This provision enables the integrator to integrate the area between the the

signal signature and any horizontal line below it. (see Fig. 3) and thus provides a way to evaluate the size distribution of the frazil flocs in the flowing water. A counter is connected to the integrator to show the area integrated. When used online, the usefulness of the integrator probably is limited to giving the total amount of frazil flowed through the sensing point over the measuring period, or the average concentration of frazil at that point over the measuring period. The greater usefulness of the integrator is for calculating the differential area between the signal and the reference voltage to evaluate the size distribution of the frazil flocs as noted above when the analog signal is refed to the integrator from playing back the tape that had been recorded earlier.

The bottom part of Fig. 3 shows the deicing component of the instrument. It was mentioned earlier that for the Phase II instrument, electrical heating was used to deice the probes and the probe supports and much difficulty was encountered with this kind of heating method. To avoid the same problems, oil heating was used in the conceptual design. It is seen from Fig. 3 that the electrode plates are embedded in oil vessels in such a way that the backs of the plates are exposed to the warm oil and the face of the plates are exposed to the water. Good seal is provided to ensure that the oil will not leak into the water and vice versa. It may be added that the probe supports are also oil heated although this is not explicitly shown in the diagram. The temperature of the oil in the probe chamber is controlled by the temperature of the returning oil. When the temperature of the returning oil is measured to be less than the preset value which is above freezing, the heater control will activate the heater in the oil reservoir to heat up the oil. For safety reasons, the temperature of the oil in the reservoir is also sensed. When the oil temperature in the reservoir is greater than the preset limit, the heater control will cut off the heater as well as the pump. In the conceptual design, a positive displacement, constant discharge pump is called for.

4.0 ELECTRONIC AND MECHANICAL DESIGN OF INSTRUMENT

According to the conceptual design, electronic circuitries and mechanical parts of the instrument were designed and constructed. Because of proprietory reasons, the detailed electronic schematics and mechanical drawings are not shown here, but issued as a separate report by the authors* and may be obtained through proper channels. Some of the vital design parameters of the instrument are given below.

1. The constant current between the electrodes of each probe is 4 mA.
2. The frequency of the AC current is 1024 Hz and the transient time of switching is 10^{-6} seconds.
3. The dimensional gain factor of the instrument is G = 51.0 volts, giving a signal voltage output of the instrument of

$$V_{sig} = 51.0 \frac{V_s - V_r}{V_r} = 51.0 \frac{R_s - R_r}{R_r} = 51.0\, c_f \qquad (24)$$

4. The range of V_{sig} is 0 to 10 volts.
5. The relationship between the counts given by the counter and the integrated area between the signal output curve and the reference voltage V_{ref} (see Fig. 3) is

$$N = \int_{\tau} \frac{(V_{sig} - V_{ref})}{0.512}\, dt \qquad (25)$$

where τ is the period of integration. The above equation may be

---

* Tsang, G. and Pedrosa, M. Electronic and mechanical designs of the NWRI Frazil Instrument. NWRI Report No. Tsang (51) Pedrosa (3), October, 1983.

rearranged to give the average value of $(V_{sig} - V_{ref})$ in the time period τ

$$\overline{(V_{sig} - V_{ref})} = \frac{0.512N}{\tau} \qquad (26)$$

6. The two probes are identically constructed although one is designated as the reference probe and the other as the sensor probe and must be always so used. Each probe is in the form of two hollow shells facing each other. The housing of the shell is machined out of plastic with a circular stainless steel plate embedded at the front to serve as the electrode. The diameter of the shell is 8.5 cm and the thickness is 1.6 cm. To avoid disturbing the flow into the probe, the shells are chamferred to have an angle of 45°. Warm oil is circulated through the chamber inside the shell by means of two stainless steel tubings which also serve as the probe support and the sheaths to shield the wires that connect the electrodes to the connector at the top of the support.
7. The diameter of the electrodes is 5 cm and the electrodes are 5 cm apart, giving a sample volume of approximately 100 cm^3.
8. The overall length of the probe and the support is 1.25 m.
9. The temperature of the returning oil is controlled to be at 7°C.
10. The temperature of the oil in the oil reservoir is controlled to be at less than 70°C.

The finished instrument, constructed mainly for laboratory use, is shown by the photograph in Fig. 4. It is seen from Fig. 4 that the instrument consists of three entities. They are the probes and their supports, on the right, the oil box that contains the warm oil, the oil temperature sensors and the pump, in the middle, and the electronic box that contains all the electronics, on the left.

5.0 CALIBRATION

5.1 The Multiplying Factor Between Theoretical and Measured Concentrations.

In the preceding section, the signal voltage output of the instrument was shown to be given by Eq. 24. The measured concentration of frazil in water, here denoted as c_{fm}, therefore, is given by

$$c_{fm} = V_{sig}/G = \frac{V_{sig}}{51.0} \tag{27}$$

The conclusion that the concentration of frazil is given by $(R_s - R_r)/R_r$ (Eq. 22) was derived assuming that frazil crystals are geometrically isotropic. In reality, this is not the case and the frazil crystals are in the shapes of discoids (mostly), needles and flakes. Because the non-isotropic shape of the frazil crystals, the electrical path between the two electrodes is longer than that if the frazil crystals were isotropic. The longer electrical path means that the resistance of the sensor probe is greater than the theoretical value or that the signal output of the instrument is larger than the theoretical signal output by a multiplying factor greater than unity. Let F be this multiplying factor and c_{ft} be the theoretical frazil concentration, from the above discussion one sees that

$$F = c_{fm}/c_{ft} \tag{28}$$

In evaluating the experimental frazil instrument during Phase I of the instrument development, Tsang (1977) found that F varied in the range of 3.06 to 5.52 with an average value of 3.44. Because of the inadequate design of the experimental instrument, close multiplying factors could not be obtained for similar experiments. As a matter of fact, the two multiplying factors from two similar

experiments often exhibited a difference as great as fifty percent. For the instrument reported here, as will be seen later, a much better defined F was obtained.

5.2 The Calibration Setup

The instrument was calibrated in a cold room the temperature of which could be set from room temperature to -30°C. The actual temperature of the cold room fluctuated about the set temperature in a skewed sinusoidal fashion with an amplitude of 1.5°C and a period of 4 minutes. A recirculating flume made of transparent plastic was constructed to facilitate the calibration. The recirculating flume and the basic calibration setup is shown in Fig. 5. It is seen from Fig. 5 that the recirculating flume was race-track shaped. It had a cross-section of 15 cm (6") wide x 13 cm (5") deep. During calibration, the flume was filled with tap water to 2 cm from the top. A variable speed propeller was mounted at one end of the flume to produce the desired current velocity. To accelerate cooling, a fan (not shown) was placed about 1.5 m from the flume which produced a wind of about 0.5 m/s over the water. The temperature of the water was measured with a precision thermometer (Guildline) that had a resolution of 0.001°C and an accuracy of 0.002°C. The air temperature in the room was measured with a less precise thermometer (Hewlett Packard, not shown) that had a resolution of 0.01°C and an accuracy of 0.02°C. To prevent frazil from being nucleated by and adhering to the sides and the bottom of the flume, the flume was embedded in a warm air jacket. Light bulbs and recirculating fans were installed in the air jacket to ensure temperature uniformity. The voltage to the light bulbs could be varied by means of a variable transformer. By manipulating the voltage to the light bulbs, the temperature of the air jacket could be maintained at from 2°C to 7°C. It is seen from Fig. 5 that while the sensor probe was placed in the mainstream of the flow in one of the straight sections of the flume, the reference probe was accommodated in a depression chamber

added to the bottom of the flume. The depression chamber was covered with two half-plates with slots cut in them for the probe supports to pass through. Because the depression chamber was surrounded by warm air, the water exchange between the mainstream and the chamber was limited by the small slots in the half-plates and the natural buoyancy of ice discourages frazil from moving down into the depression chamber, the water temperature in the chamber was measured to be near that of the main stream and no frazil was observed in the chamber during the calibration.

Fig. 6 shows the monitoring and recording system of the calibration. It is seen from Fig. 6 that the air temperature was measured with a Hewlett Packard HP34750A thermometer and recorded on a Hewlett Packard HP7100B chart recorder. The water temperature was measured with a Guildline G9535 thermometer and was also recorded on the HP7100B chart recorder when the water temperature was in the coarse range of 4.0 to -2.0^{o}C. When the water temperature entered into the fine range of .25 to -.25^{o}C, however, it was also recorded on a more precise Gould 2400 brush chart recorder. Before the temperature voltage was recorded on the Gould recorder, however, it was amplified 50 times for the temperature voltage to be simultaneously recorded by a Hewlett Packard HP3960 tape recorder. The reason for doing this was because the input voltage range of the HP3960 tape recorder selected for channel 1 was from -2.5 to 2.5V. To fully utilize this voltage range, the voltage range of -50mV to 50 mV produced by the Guildline thermometer, corresponding to a temperature range of -.25 to -.25^{o}C, should be amplified by a factor of 50.

Besides the -2.5 to 2.5V range, two other ranges, namely -5.0 to 5.0V and -10.0 to 10.0V might also be selected for the HP3960 tape recorder when recording signals. Because the nominal output voltage range of the tape recorder was -2.5 to 2.5V, the above selection of input voltage ranges when recording means that when the -2.5 to 2.5 V range was used, the signal voltage would be undistortedly recorded, when the -5.0 to 5.0 V range was used, the signal voltage would be

compressed to 50% and when the -10.0 to 10.0 Vrange was used, the signal voltage would be compressed to 25%.

The voltage signal from the frazil instrument was also both chart and tape recorded. It is seen from Fig. 6 that the 5 V range of the Gould chart recorder was used in recording the frazil signal. Because the output range of the frazil instrument was 0 to 10 V, using the 5 V range although would produce a more readable chart, especially when the concentration of frazil was small, the output signal greater than 5 V would be missed by the recorder. To remedy this problem, when tape recording the frazil signal, the voltage was compressed to 25% before being recorded in channel 4. With such a compression, the output voltage range of the frazil instrument was compressed from 0 to 10 V to 0 to 2.5 V to match the positive half of the voltage range of the tape recorder.

The frazil signal was also compressed to 50% and recorded in channel 3 of the tape. This additional recording would on one hand provide a check to the recording in channel 4, and on the other hand, when played back to the chart recorder using the 2.5 V range, reproduce a chart recording identical to the one obtained when monitoring the experiment as further verification.

Channel 2 of the tape recorder was not used for information recording, instead, it was used for fluttering, or compensation of high and low frequency noises generated internally in the tape recorder.

5.3 Experiments and Analysis of Experimental Results

A total of five experiments were conducted for the calibration. The parameters of the calibration experiments are summarized in Table 1. It is seen from Table 1 that three experiments (Tests 1, 2 and 3) were conducted for a slow flow velocity of approximately 15 cm/s and two experiments (Tests 4 and 5) were conducted for a fast flow velocity of approximately 21.4cm/s. It should be noted that these velocities were measured before frazil was produced in the

flume. Following the formation of frazil in the flume, the flow velocity was visibly reduced although the propeller setting was maintained the same. The velocity of the frazil laden flow was not measured because presently no technique is available for measuring the velocity of a frazil laden flow. For all experiments except Test 5, frazil was produced in the flume by seeding the water with ice particles scraped from a slab of ice with a saw blade when the water was supercooled to $-.03^{o}C$. For Test 5, frazil was produced spontaneously before the water temperature reached that value.

The typical experimental result of the calibration experiments is shown by Fig. 7, which was obtained from tracing the early part of the strip chart obtained during Test 2. It is seen from Fig. 7 that the water temperature was recorded on the upper part of the strip chart and the frazil concentration signal was recorded on the lower part. The 5 V range was used for both channels. With this voltage range, the upper channel was adjusted to record the water temperature from $+.25$ to $-.25^{o}C$ and the lower channel was adjusted to record a frazil concentration from 0 to approximately 10 percent (see Eq. 29). It is seen from Fig. 7 that when the water temperature was above freezing, a slow chart speed of 0.5 mm/s was used. With a roughly constant environment, it is seen from the diagram that the cooling of the water was approximately linear with a cooling rate of about 4.975×10^{-4} °C/s. As the water temperature approached the freezing point, the chart speed was increased to 2 mm/s to give a more readable frazil concentration recording. Both static ice and frazil were not observed in the flume after the water temperature had passed the freezing point and the water become supercooled. The lower channel of the strip chart also showed no frazil was detected by the frazil instrument. When the water temperature reached $-.03^{o}C$, the supercooled water was seeded. Immediately following seeding, frazil crystals were seen in the flume. The frazil crystals grew and agglomerated into clusters which became bigger and densier (containing more frazil) with time. As soon as frazil was seen in the flume, it was also detected by the instrument as shown by the lower recording of

Fig. 7. The recording also reflects the growth and agglomeration of the frazil crystals and clusters Every time a frazil floc passed through the sensor probe, a spike was recorded. The thicker the floc, the higher was the spike. The frazil instrument, thus was seen to be working. What remained was to calibrate the instrument.

Calibration means comparing the measured concentration with the theoretically calculated concentration. The theoretical frazil concentration can be calculated from the temperature recording. From thermodynamic considerations, Tsang (1983) showed that the average concentration of frazil at time t is given by

$$c_{ft} = \frac{c}{0.961\ H_L} \left[- \left(\frac{dT}{dt}\right)_n (t - t_n) + (T - T_n) \right] \qquad (29)$$

where c is the specific heat of water, H_L is the latent heat of fusion of ice, T is the water temperature, dT/dt is the cooling rate of water, the subscript n indicates the instant of seeding and the constant 0.916 converts the mass concentration to volumetric concentration. With the above equation, if the pre-supercooling cooling rate of the water was approximately used for $(dT/dt)_n$, then from the temperature recording the theoretical frazil concentration at different instants could be calculated. The theoretical frazil concentration for the five calibration experiments at different instants is shown in Table 1. During the calculations, the time at which the temperature curve intersects the time axis was considered as time zero. It is seen from Table 1 that for all calculations, the time interval between two successive concentrations was 50 seconds except when the first three points were involved As may be seen from Fig. 7 that the first point was the time zero point, the second point was the seeding point at which the concentration of frazil would be zero and the third point was usually chosen to be the first intersection of the thicker grid line(marking 10 cm distances) with the temperature curve. The length of the centre line of the calibration flume was about 2 m.

With a flow velocity of 15.0 cm/s and 21.4 cm/s, in 50 seconds, the frazil laden water would have flowed through the sensor probe 3.75 and 5.35 times respectively.

To obtain the measured average concentrations of frazil corresponding to the calculated theoretical concentrations mentioned above, the tape-recorded frazil concentration voltage signal was played back to the instrument. Only the voltage signal recorded by channel 3 of the recorder was used in playing back. It was found from playing back the recorded signal that the signal output range of the instrument during calibration was adequately accommodated by the recording range of channel 3 if the built-in tolerance of the tape recorder was used (The voltage range of channel 3 of the HP3960 tape recorder was actually roughly -3.0/3.0 V instead of the nominal -2.5/2.5 V). With the tape-recorded input fed to the instrument, the instrument output was first examined in a voltmeter. It is seen in Fig. 7 that before frazil was produced in the water, there was a finite output from the instrument. Although this finite output could be zeroed by adjusting the "zero" potentiometer of the instrument during the experiments, this was not done to permit the observation of the meandering of the baseline, which was found to be $\pm$ 0.5 mm, representing a baseline voltage fluctuation of $\pm$ 25 mV. After the baseline voltage immediately preceeding seeding was measured and noted, a reference voltage source with a generated voltage equal to the baseline voltage was connected to the frazil instrument (see Fig. 3). The voltage signal to be integrated by the difference integrator of the instrument then became the net voltage between the recorded voltage and the baseline voltage, or the voltage produced by frazil presence only.

The integration of the above voltage produced counts. By feeding the counting signal to the event marker of the chart recorder, the counts were marked on the margin of the strip chart for later evaluation of the concentration of frazil.

Fig. 8 is an example of the strip charts with concentration counts reproduced by feeding the tape-recorded signal (on channel 3)

back to the frazil instrument. The same time period of Test 2 is shown by Figs. 7 and 8. The outward appearance of these two recordings however, is different because Fig. 8 was produced with a chart speed of 5mm/s, two and a half times the chart speed that produced Fig. 7. The amplitude of the spikes in Fig. 8 is also only half that of the corresponding spikes in Fig. 7. This is because when the output signal from the frazil instrument was tape-recorded in channel 3 of the HP3960 tape recorder, the signal voltage was compressed to 50%.

The average measured frazil concentration for the periods shown in Fig. 8 could be obtained by counting the counts shown in the periods. By comparing Figs. 7 and 8, one sees that the mid-points of the periods shown in Fig. 8 correspond to the same points shown in Fig. 7 for which theoretical frazil concentration was calculated.

According to Eq. 26, one sees that the average output voltage signal of the instrument for time period τ is given by

$$\overline{V}_{sig} = \frac{0.512N}{\tau} \quad \text{volts} \tag{30}$$

However, when the counts were reproduced by feeding the Channel 3 tape-recorded signal back to the frazil instrument, because the signal voltage had been compressed to 50%, the counts produced would only be half the original counts. To compensate for this compression effect, in calculating the actual average signal voltage of the instrument, Eq. 30 was modified to

$$\overline{V}_{sig} = \frac{.512(2N)}{\tau} \quad \text{volts} \tag{31}$$

After the average signal voltage was obtained, the division of $\overline{V}_{sig}$ by G = 51.0 volts according to Eq. 27 gave the measured average frazil concentration for the period. The measured average frazil concentration for the different periods of the five calibration experiments are

also shown in Table 1. It should be noted that in obtaining the measured concentrations of frazil with the above method, an assumption has been made that the amount of frazil passing through the probe during the 50 second period was the same as the average amount of frazil in the flume during that period.

5.4 Calibration Results and Discussion

According to Table 1, the measured concentration of frazil c_{fm} was plotted against the calculated theoretical concentration c_{ft} as shown in Fig. 9. It is seen from Fig. 9 that for all the five calibration tests, seeing the turbulent nature of the flow and the non-uniformity nature of frazil distribution in the flow because the flocking and agglomeration, the relationships between c_{fm} and c_{ft} were surprisingly linear. The slopes of the five fitting straightlines fitted with the method of least squares are shown in Fig. 9. as well as listed in Table 2.

It is seen from the Table 2 that the calibration multiplying factor of the instrument was affected by the velocity of the flow. However, for a given velocity, the multiplying factor was not affected by the air temperature, which determined the rate of frazil formation, nor by the amount of frazil present in the water. When the flow velocity was in the 15-16 cm/s range, Tests 1, 2 and 3 showed that the multiplying factor varied from 3.560 to 3.885 with a mean of 3.733, giving a deviation from the mean of less than 5 percent. When the flow velocity was 21.4 cm/s, Tests 4 and 5 showed that the multiplying factor was 2.538 and 2.207 respectively with a mean of 2.373. The deviation from the mean was less than 7 percent. The decrease of F with the increase of flow velocity was apparent. As the velocity increased from about 15 cm/s to 21.4 cm/s, the mean F value decreased from 3.723 to 2.373. Even for the first three tests, it is seen from Table 2 that as the flow velocity changed from 15.0 to 15.6 to 16.0cm/s, the multiplying factor decreased from 3.885 to 3.756 to 3.560 respectively.

The large multiplying factor for slower flow velocities was not because the change of the response of the frazil instrument to ice presence, but the change of the agglomeration characteristics of the frazil and consequently the flow characteristics of the frazil/water mixture because of the slower flow. It was observed during the experiments that when the flow was slow, the frazil floc would be sluggish in passing through the sensor probe because of insufficient momentum possessed. The slow passage of the frazil flocs through the sensor probe means that the frazil flocs had a longer resident time in the probe and hence gave a seemingly higher concentration. During the experiments, it was observed that occasionally large flocs would even be caught by the probe and would only be dislodged when the probe was lightly tapped by hand. For this reason, during the experiments, the support of the sensor probe was constantly tapped. As the flow velocity increased, the frazil flocs possessed greater momentum and was seen passing through the probe smoothly. The slow passage of frazil flocs through the sensor probe when the flow velocity was low was further aggravated by the larger size and the thicker flocs of the frazil agglomeration. When the flow was slow, because the turbulence level was low, the frazil crystals were able to agglomerate into bigger and thicker flocs or clusters. When the flow velocity was increased, the higher turbulence tended to break up the agglomeration into smaller and more evenly distributed flocs. The above can indeed be seen from comparing Fig. 10, which is the frazil concentration recording of Test 4 obtained by playing back the Channel 3 tape recorded signal to the instrument, with Fig. 8. It is seen from Table 1 that these two calibration tests (Test 2 and Test 4) had about the same rate of heat loss so the concentration of frazil for the shown time period should be similar. However, a comparison of the two recordings shows that the 16.0 cm/s flow produced larger and denser flocs than those produced by the 21.4 cm/s flow. The latter also exhibits more evenly distributed frazil flocs and less concentration fluctuations within the flocs themselves as evidenced by the rather evenly distributed ticks marked by the event marker. Since

turbulence affects the agglomeration characteristics of frazil, any factor that affects turbulence therefore is also a potential factor in influencing the calibration factor.

It follows from the above discussions that if the flow velocity is sufficiently high, an asymptotic F value will be approached. This asymptotic multiplying factor will be the real multiplying factor of the frazil instrument because of the anisotropy of the frazil crystals. From the experiments, it can be seen that this real multiplying factor would be less than the least multiplying factor of 2.207 obtained. However, it should not be too far less than this value because it was observed during Test 5 that at 21.4 cm/s the frazil flocs flowed through the sensor probe with ease.

A turbulence dependent coefficient may be introduced to account for the turbulence effect on the multiplying factor. In mathematical terms, this means writing

$$F = c_t F_r \tag{34}$$

where F_r is the real multiplying factor and c_t is the turbulence correction coefficient. To establish the value of F_r and the functional relationship between C_t and turbulence is beyond the scope of the present report. At this point, it will be sufficient to say that with the present calibration set up, the multiplying factor F for a reasonable flow velocity (and hence turbulence) range can be evaluated if needed.

7.0 CONCLUSIONS AND SUMMARY

The development and calibration of the frazil instrument can be summarized as follows:

1. The proposed theory shows that the concentration of frazil in water can be measured by measuring $(R_s - R_r)/R_r$, where R_s is the electrical resistance of a sample of frazil laden water

between two electrodes and R_r is the resistance of an identical sample of frazil free water.

2. Electronic circuitry and mechanical parts were designed and an instrument to measure the above parameter was constructed.
3. The newly developed frazil instrument was laboratory-calibrated in a recirculating flume. The calibration showed that the instrument performed satisfactorily.
4. Because of the non-isotropic shape of the frazil crystals and the flow characteristics of the frazil flocs, the measured frazil concentration has to be corrected with a multiplying factor F to obtain the true frazil concentration. The calibration experiments showed that F is not affected by the quantity of frazil in the water, nor by the rate at which frazil is produced. However, it is a function of the velocity of the flow.
5. F is affected by the flow velocity because the flow velocity determines the momentum of the frazil flocs and the turbulence level of the flow and the latter, in turn, affects the agglomeration characteristics of the frazil.
6. The multiplying factor of the instrument may be considered as composing of two parts, $F = c_t F_r$, where F_r is the multiplying factor because of the non-isotropic shape of the frazil crystals and c_t is the correction coefficient because of flow velocity and turbulence. F_r should be smaller, but close to 2.2.
7. The F value for a flow velocity of 15-16 cm/s was found to be 3.723 and the F value for the flow velocity of 21.4 cm/s was found to be 2.373. The F value for flow velocity less than about 22 cm/s can be obtained by calibrating the instrument with the calibration setup mentioned in this report. For first order approximation, it may be obtained by interpolation of the values shown above.

7.0 ACKNOWLEDGEMENT

The assistance of Mr. Paul Carney is gratefully acknowledged for his design and construction of the mechanical parts.

9.0 REFERENCES

Ford, J.S., (1982). "An Engineering Proposal For a Frazil Recorder". Technical Note. No.E82-02, Hydraulics Division, National Water Research Institute, Burlington, Ontario. February.

Ford, J.S., Der, C.Y., Mollon, K., and Roy, F., (1981). "Progress Report on Analyses and Laboratory Tests for a Frazil Ice Sensor". Internal Report No. EPR-01. Engineering Services Section, Hydraulics Division, National Water Research Institute, Burlington, Ontario. March.

Gilfilian, R.E., Line, W.L., and Osterkamp, T., (1972). "Ice Formation in a Small Alaskan Stream". UNESCO-5: Properties and Process of River and Lake Ice.

Kristinsson, B., (1970). "Ice Monitoring Equipment". Proc. IAHR Symp on Ice and Its Action on Hydraulic Structures, Reyjavik, Sept. pp. 1-1-14.

Schmidt, C.C., and Glover, J.R., (1975). "A Frazil Ice Concentration Measuring System Using a Laser Doppler Velocimeter". Journal of Hydraulic Research, IAHR, Vol. 13, No. 3, pp. 299-314.

Tsang, G., (1974). "Conceptual Design of a Multi-purpose Instrument for Winter Stream Metering". Proc. of International Symp. on Advanced Concepts and Techniques in the Study of Snow and Ice Resources. Monterey, December, 1973, Published by the U.S. Nat. Acad. of Sciences, pp 688-698.

Tsang, G., (1977) "Development of an Experimental Frazil Ice Instrument". Proc. of 3rd Nat. Hydrotechnical Conf., Quebec, May, pp.671-692.

Tsang, G., (1982) "Frazil Ice Instrument Development Phase II - Progress Report", Unpublished Report, Hydraulics Division, Nat. Water Res. Inst., CCIW, Burlington, Ontario. May.

Tsang, G., (1983) "Formation and Properties of Frazil Formed in Seawater at Different Supercoolings". Proc. of Conf. of Port and Ocean Engineering under Arctic Conditions (POAC '83), Helsinki, April, in press.

FIGURES AND TABLES

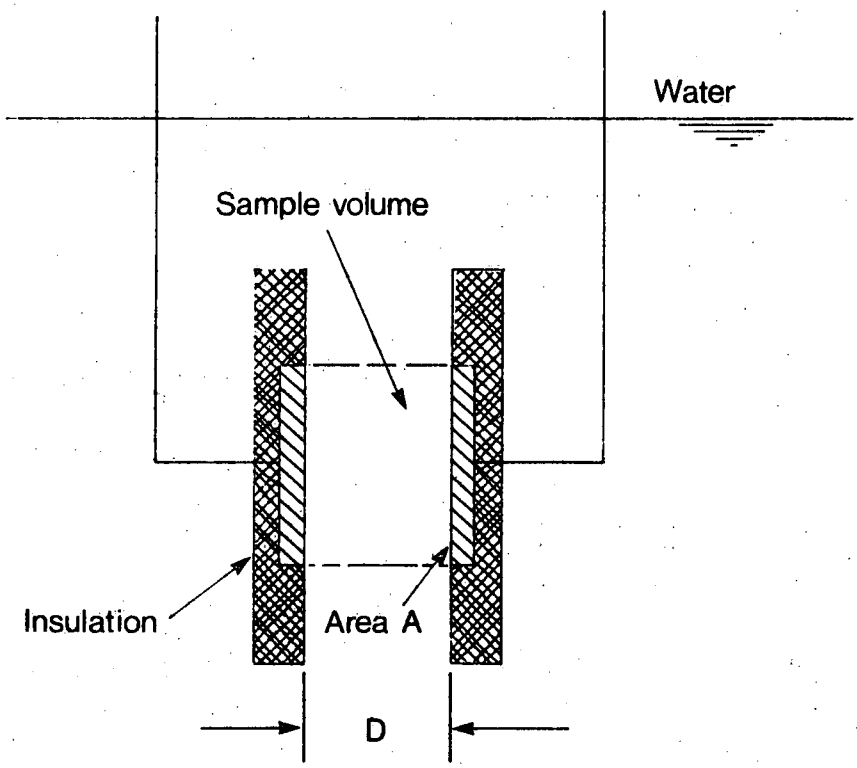

Fig. 1 Resistance between Two Insulated Plates

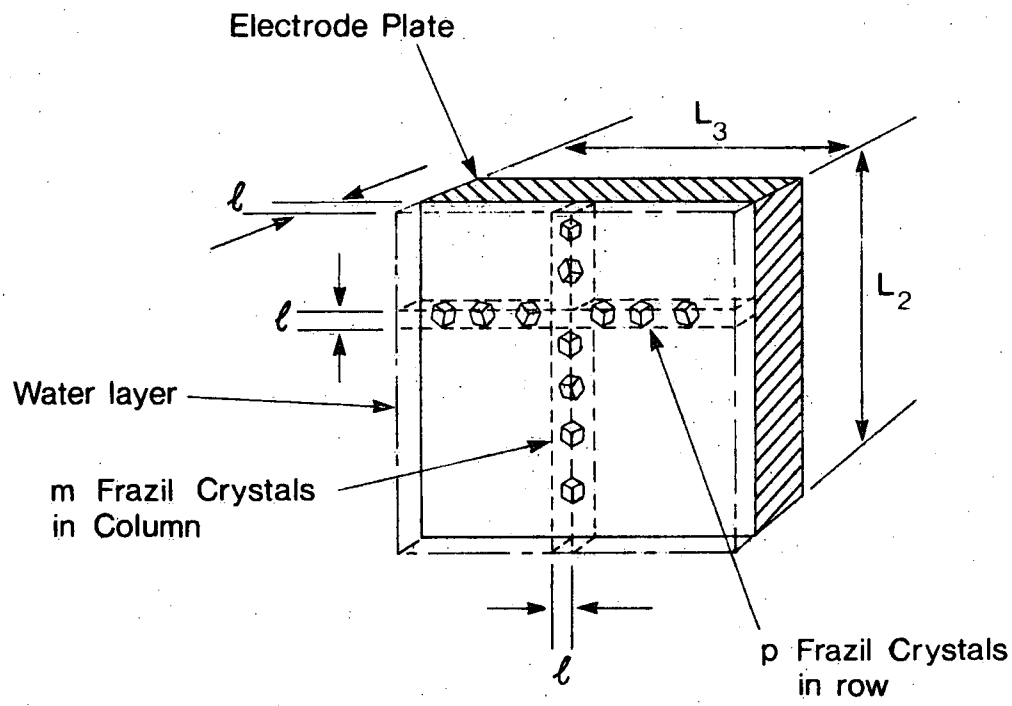

Fig. 2 Blockage of Electrical Line Receiving Area of Electrode Plate by Frazil Crystals

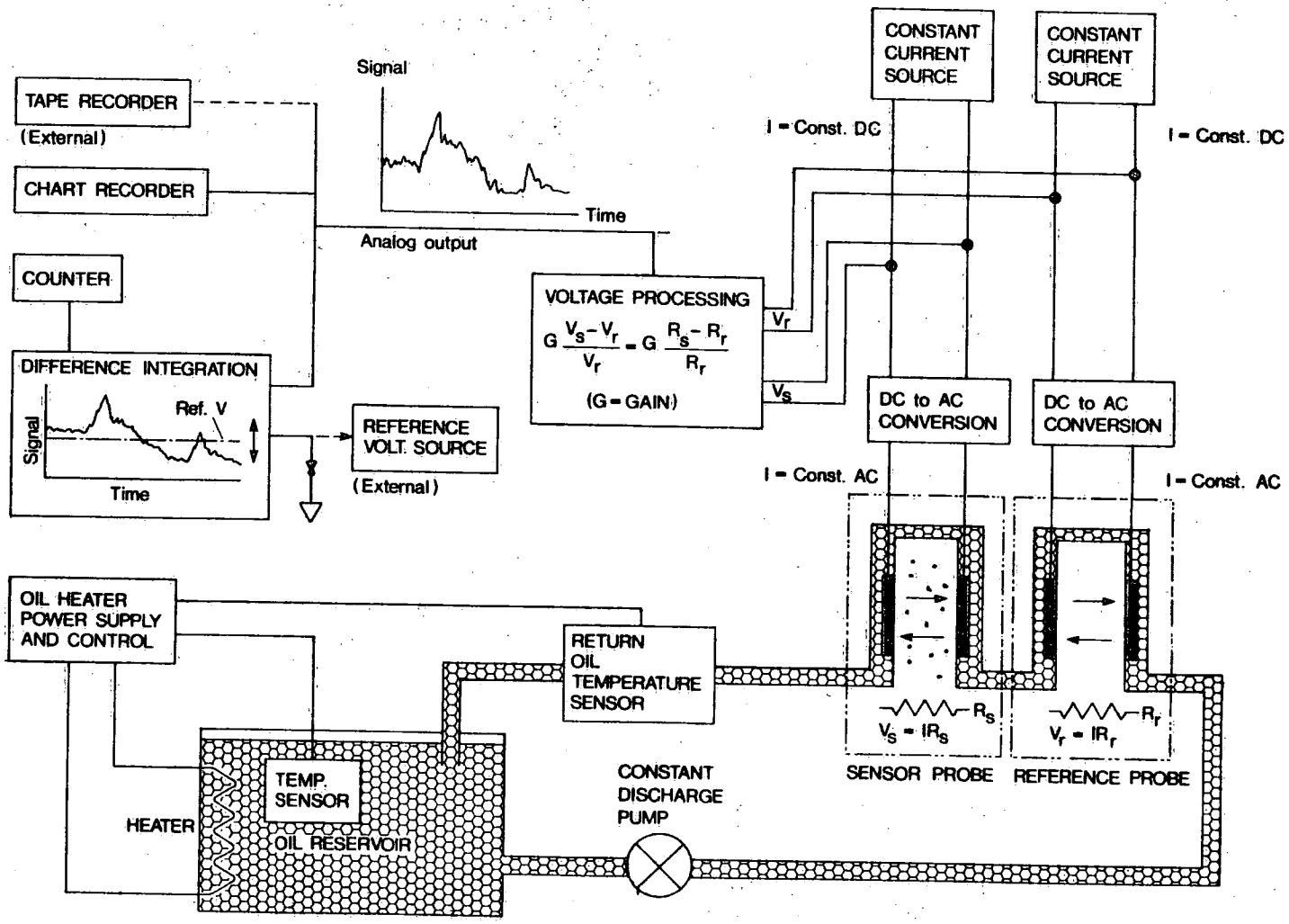

Fig. 3 CONCEPTUAL DESIGN OF FRAZIL INSTRUMENT

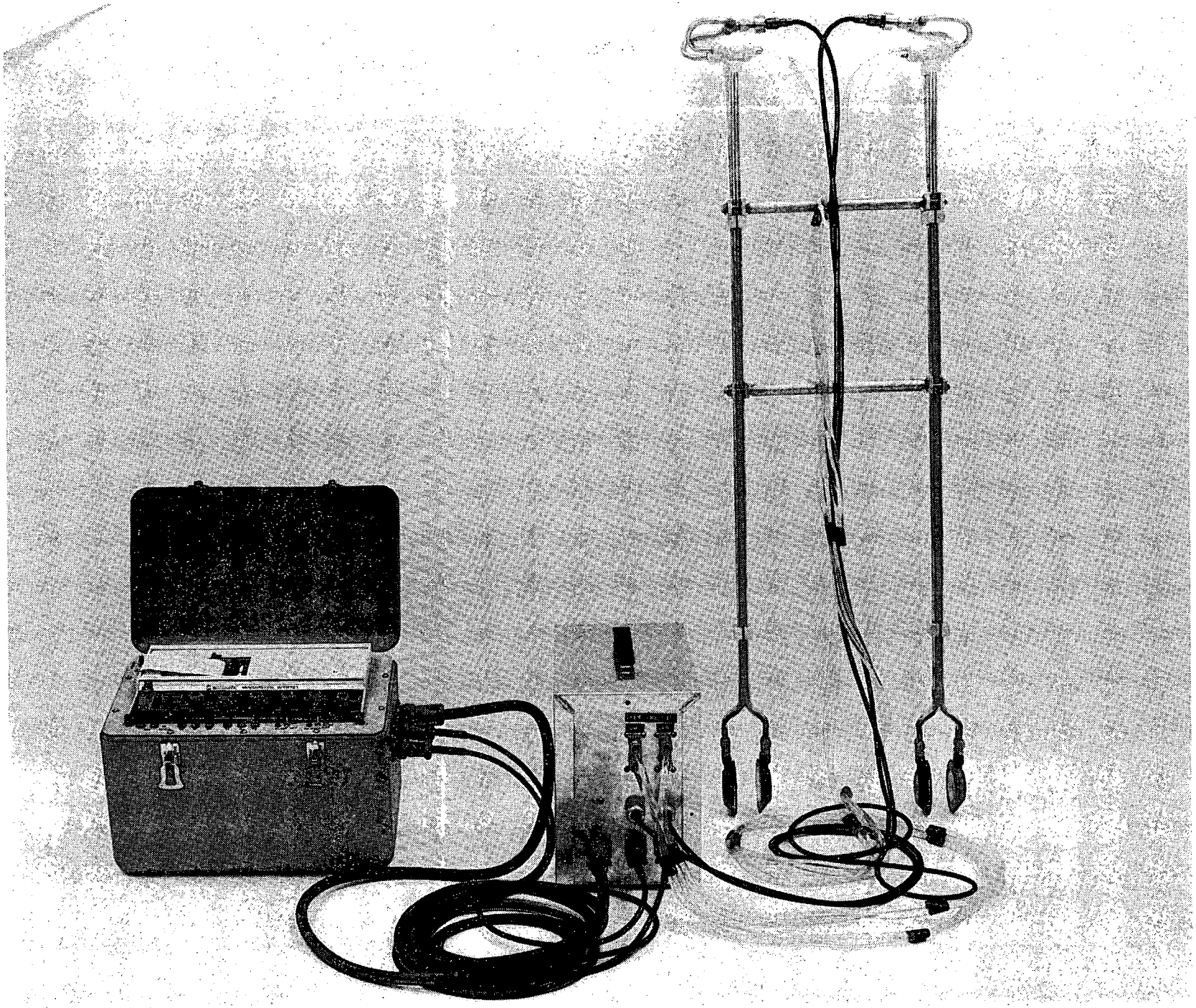

Fig. 4 NWRI Frazil Instrument for Laboratory Use

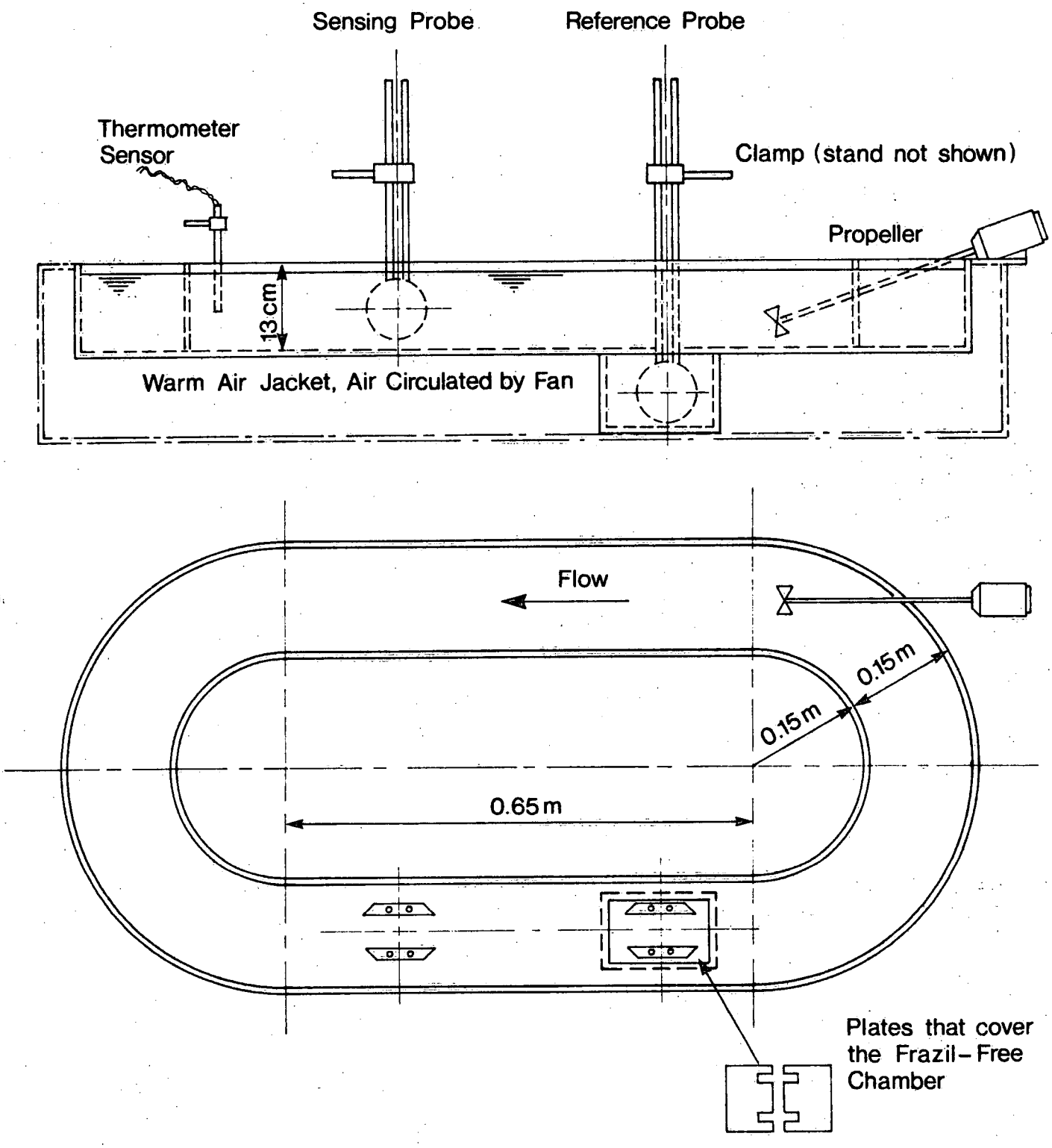

Fig. 5 Calibration Recirculating Flume and Calibration Setup

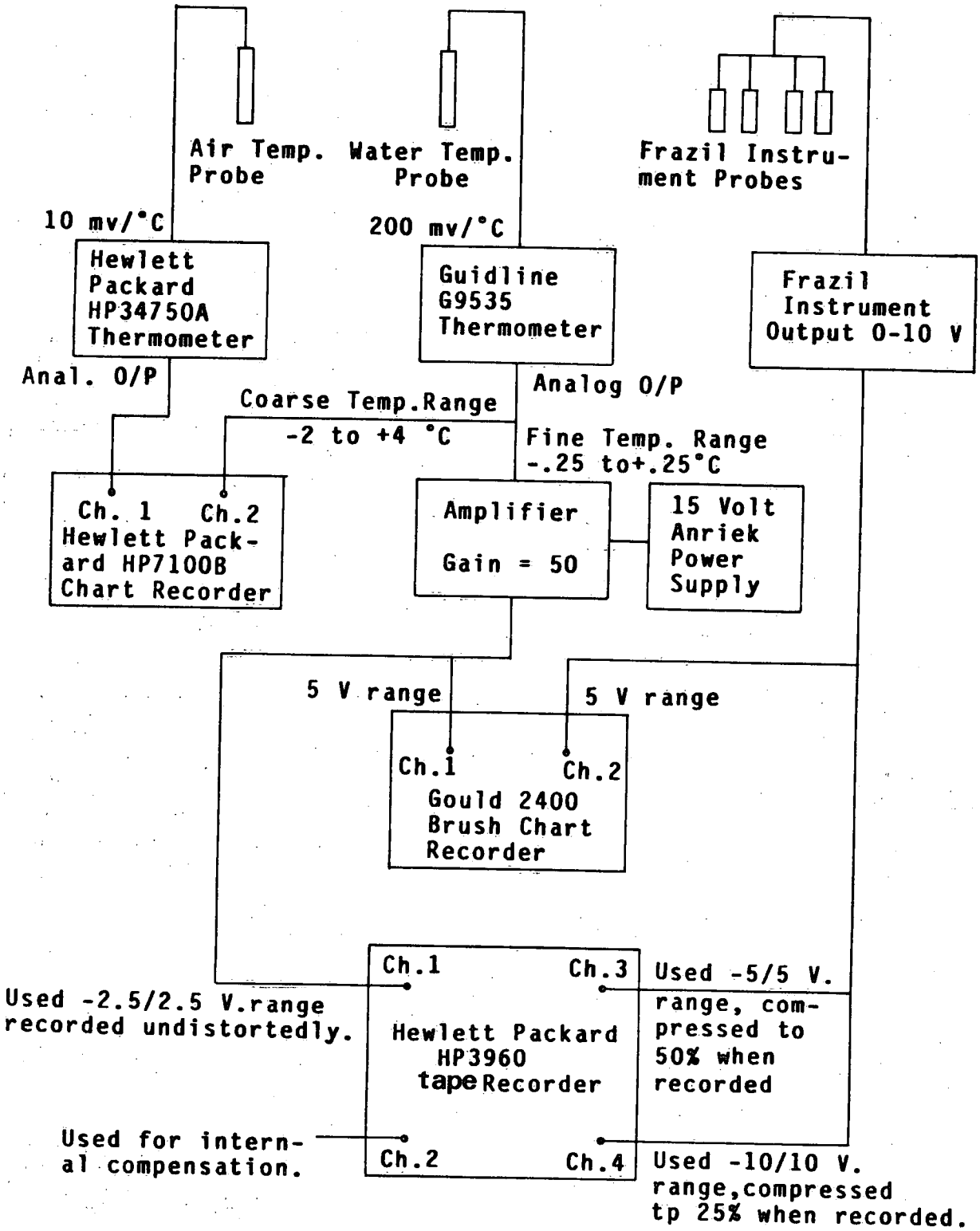

Fig.6 Calibration Monitoring and Data Acquisition System.

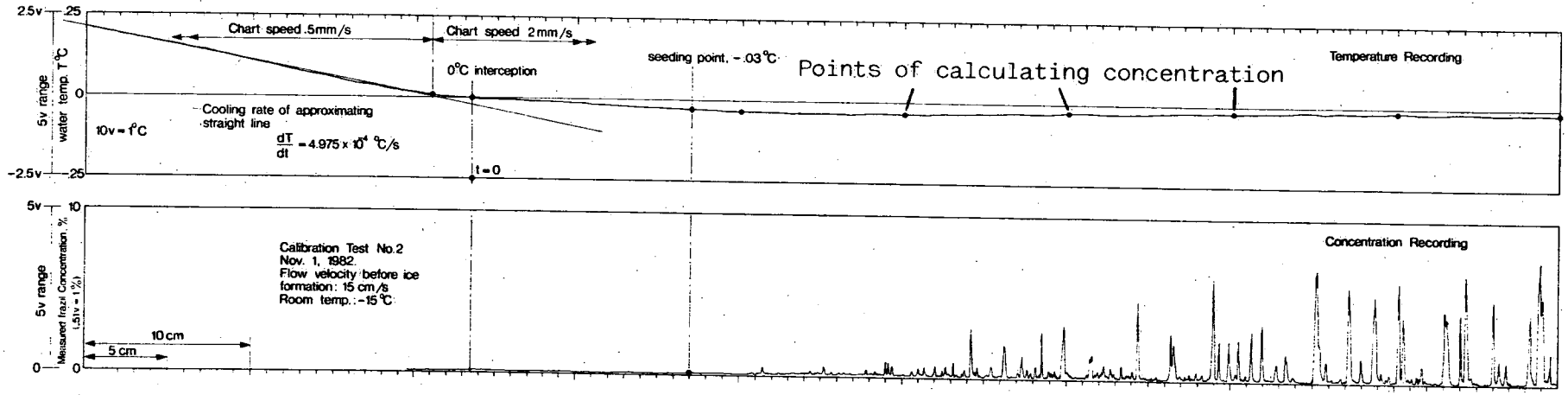

Fig. 7 Experimental Recording for the Early Part of Test 2

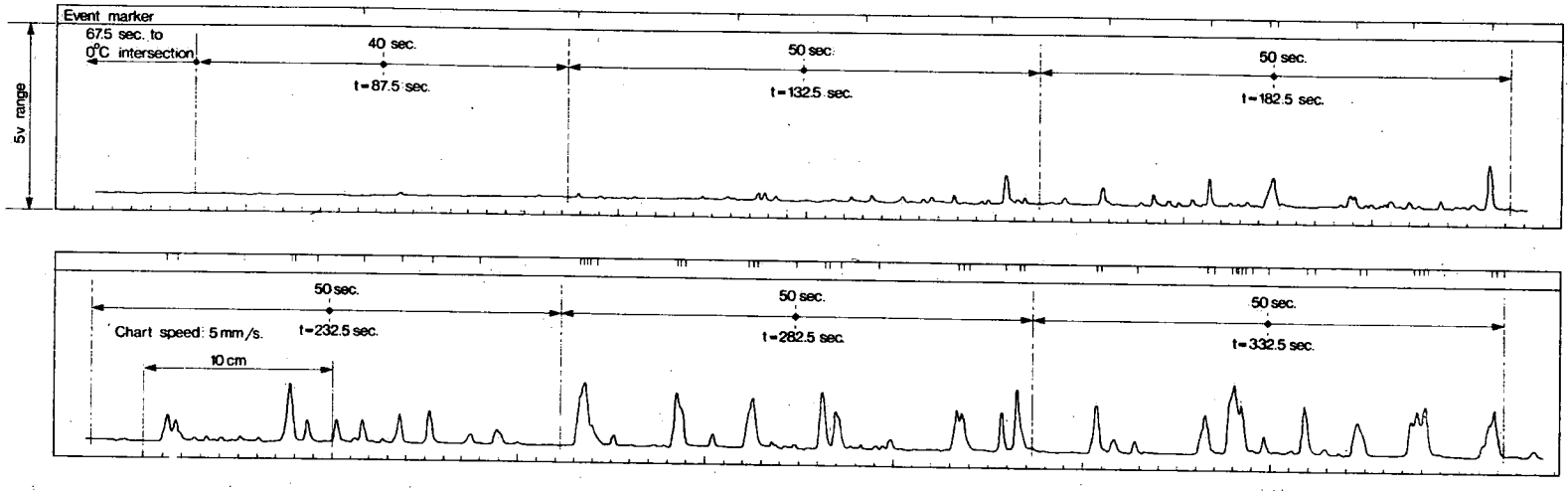

Fig. 8 Frazil Concentration Recording Reproduced by Feeding Tape Recorded Signals Back to the Instrument (Test 2)

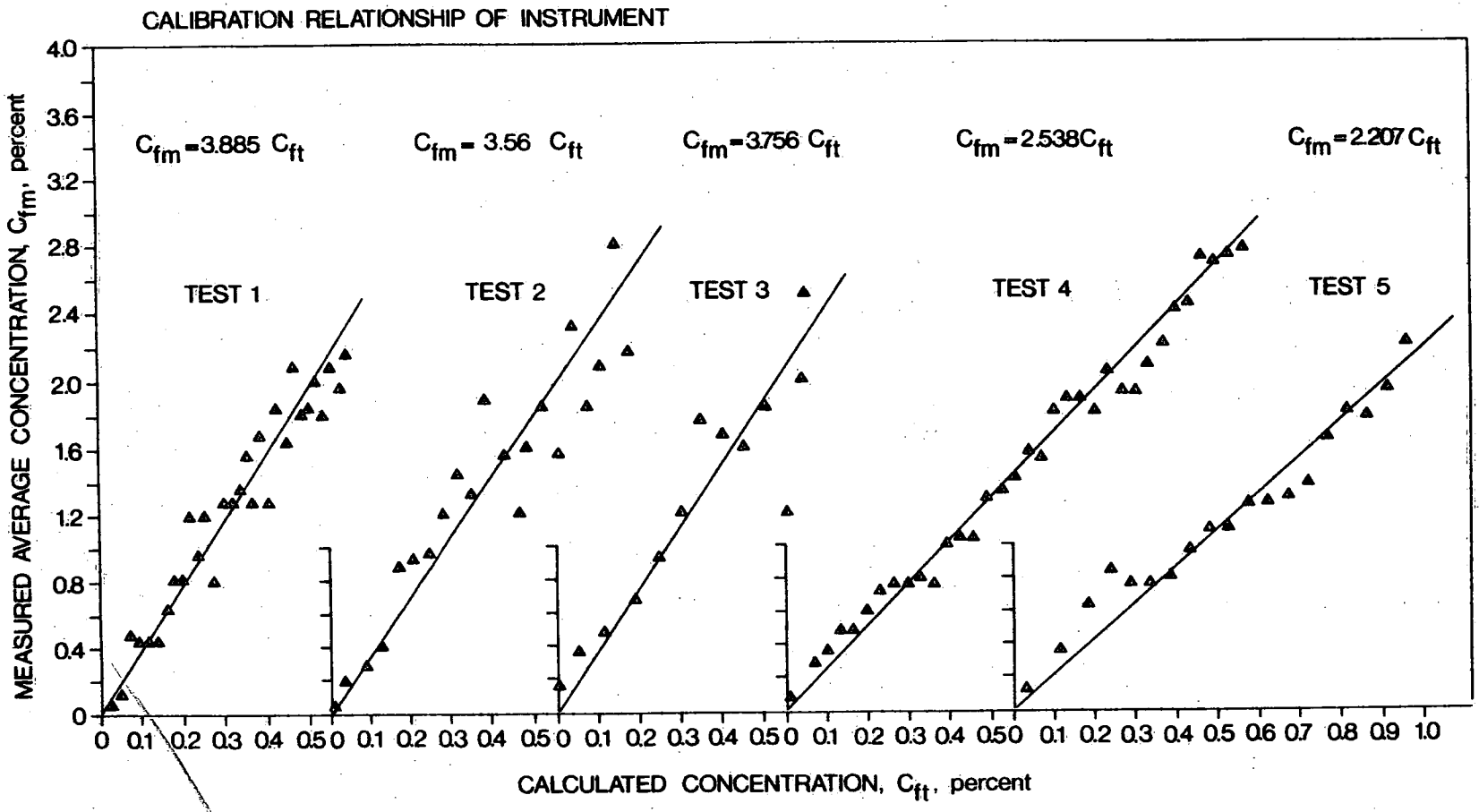

Fig. 9 Calibration Relationship of Instrument

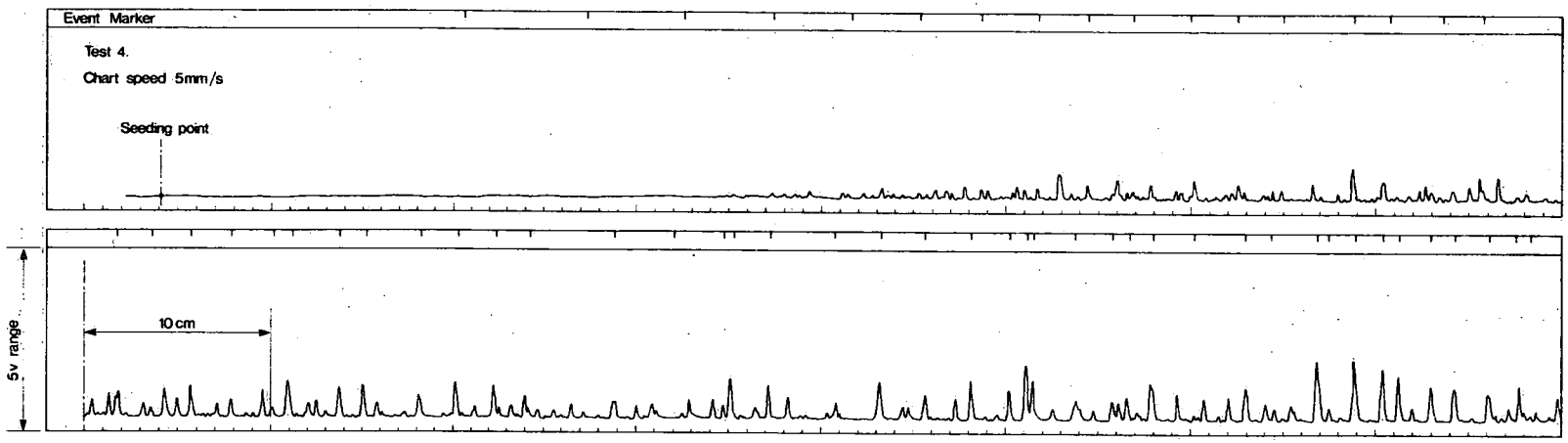

Fig. 10 Frazil Recording of Test 4 Reproduced by Feeding Tape Recorded Signals Back to the Instrument

TABLE 1. SUMMARY OF CALIBRATION EXPERIMENTS

Test No.	1	2	3	4	5
Flow Velocity before Ice V cm/s	15.0	16.0	15.6	21.4	21.4
Air Temperature T_a °C	-10	-15	-20	-15	-20
Cooling Rate of Water at Seeding $(dT/dt)_n$ 10^{-4} °C/s	2.707	4.975	7.350	4.670	6.848
Seeding Temperature T_n °C	-.030	-.030	-.030	-.030	Spontaneous Nucleation
Conductivity of Water P μmho/cm	210	-	285	263	200

Time from 0°C t sec.	Calc. Concent. c_{ft} %	Measured Conc. c_{fm} %	t	c_{ft}	c_{fm}	t	c_{ft}	c_{fm}	t	c_{ft}	c_{fm}	t	c_{ft}	c_{fm}
121.5	0.000	0.00	67.5	0.000	0.00	42.0	0.000	0.00	65.0	0.000	0.00	67.0	0.000	0.00
191.5	0.023	0.06	87.5	0.009	0.04	67.5	0.003	0.16	95.0	0.011	0.08	117.0	0.027	0.12
241.5	0.047	0.12	132.5	0.035	0.20	117.5	0.054	0.36	145.0	0.068	0.28	167.0	0.110	0.36
291.5	0.072	0.48	182.5	0.086	0.28	167.5	0.112	0.48	195.0	0.099	0.36	217.0	0.178	0.64
341.5	0.092	0.44	232.5	0.127	0.40	217.5	0.190	0.68	245.0	0.130	0.48	267.0	0.232	0.84
391.5	0.115	0.44	282.5	0.170	0.88	267.5	0.247	0.92	295.0	0.161	0.48	317.0	0.280	0.76
441.5	0.135	0.44	332.5	0.206	0.92	317.5	0.302	1.20	345.0	0.193	0.60	367.0	0.327	0.76
491.5	0.158	0.64	382.5	0.246	0.96	367.5	0.351	1.76	395.0	0.227	0.72	417.0	0.373	0.80
541.5	0.178	0.82	432.5	0.280	1.20	417.5	0.405	1.68	445.0	0.261	0.76	467.0	0.422	0.96
591.5	0.197	0.82	482.5	0.314	1.44	467.5	0.451	1.60	495.0	0.294	0.76	517.0	0.468	1.08
641.5	0.215	1.20	532.5	0.349	1.32	517.5	0.503	1.84	545.0	0.325	0.80	567.0	0.513	1.08
691.5	0.234	0.96	582.5	0.383	1.88	567.5	0.556	1.20	595.0	0.358	0.76	617.0	0.561	1.24
741.5	0.252	1.20	632.5	0.429	1.56	607.5	0.593	2.00	645.0	0.390	1.00	667.0	0.608	1.24
791.5	0.272	0.80	682.5	0.463	1.20	672.5	0.598	2.50	695.0	0.422	1.04	717.0	0.655	1.28
841.5	0.296	1.28	732.5	0.484	1.60				745.0	0.453	1.04	767.0	0.703	1.36
891.5	0.315	1.28	782.5	0.519	1.84				795.0	0.485	1.28	817.0	0.751	1.64
941.5	0.334	1.36	832.5	0.558	1.56				845.0	0.520	1.32	867.0	0.798	1.80
991.5	0.352	1.56	882.5	0.593	2.32				895.0	0.555	1.40	917.0	0.846	1.76
1041.5	0.366	1.28	932.5	0.628	1.84				945.0	0.587	1.56	967.0	0.893	1.92
1091.5	0.385	1.68	982.5	0.658	2.08				995.0	0.618	1.52	1017.0	0.940	2.20
1141.5	0.404	1.28	1032.5	0.696	2.80				1045.0	0.649	1.80			
1191.5	0.424	1.84	1082.5	0.727	2.16				1095.0	0.680	1.88			
1241.5	0.447	1.64							1145.0	0.713	1.88			
1291.5	0.466	2.08							1195.0	0.746	1.80			
1341.5	0.484	1.80							1245.0	0.780	2.04			
1391.5	0.500	1.84							1295.0	0.812	1.92			
1441.5	0.518	2.00							1345.0	0.845	1.92			
1491.5	0.536	1.80							1395.0	0.875	2.08			
1541.5	0.554	2.08							1445.0	0.910	2.20			
1591.5	0.578	1.96							1495.0	0.940	2.40			
1641.5	0.595	2.16							1545.0	0.971	2.44			
									1595.0	1.002	2.72			
									1645.0	1.035	2.68			
									1695.0	1.068	2.72			
									1745.0	1.102	2.76			

Notes:
1. The temperature at which the conductivity of water was measured for Tests 1, 3, 4 and 5 was 6.0, 18.8, 12.0 and 5.0 °C respectively. The same water was used for both Tests 2 and 4.
2. The wind velocity over the flume was about 0.5 m/s.
3. For Test 5, frazil was observed before water temperature reaching -.030 °C.
4. The averaging time for calculating frazil concentration was 50 seconds for all tests.

Table 2. Calibration Coefficients of Instrument

Test No.	1	2	3	4	5
Flow velocity before ice, cm/s	15.0	16.0	15.6	21.4	21.4
Air temperature, ^{o}C	-10.0	-15.0	-20.0	-15.0	-20.0
Calibration factor, $F = c_{fm}/c_{ft}$	3.885	3.560	3.756	2.538	2.207
Average F		3.733		2.373	
Turbulence correction coefficient c_t	1.77	1.62	1.71	1.15	1.00